Journal of The Electrochemical Society, **152** (11) C751-C755 (2005)
0013-4651/2005/152(11)/C751/5/$7.00 © The Electrochemical Society, Inc.

Formation of HgSe Thin Films Using Electrochemical Atomic Layer Epitaxy

Mkhulu K. Mathe,[a] Steve M. Cox,[b] Venkatram Venkatasamy,[a] Uwe Happek,[b] and John L. Stickney[a,*,z]

[a]*Department of Chemistry, and* [b]*Department of Astronomy and Physics, University of Georgia, Athens, Georgia 30602, USA*

The growth of HgSe using electrochemical atomic-layer epitaxy (EC-ALE) is reported. EC-ALE is the electrochemical analog of ALE, where electrochemical surface-limited reactions referred to as underpotential deposits, generally result in the formation of an atomic layer of an element, under controlled potential. HgSe thin films were formed on gold substrates using two reactant solutions: a solution of Hg^{2+} complexed with ethylenediaminetetraacetic acid and a $HSeO_3^-$ ion solution. X-ray diffraction analysis showed a zinc blende structure for the deposits, with a strong (111) preferred texture, and an average grain size of 425Δ. Electron probe microscope analysis showed near-stoichiometric deposits. Fourier transform infrared spectroscopy reflection absorption measurements suggest two bandgaps: 0.42 and 0.88 eV.
 [DOI: 10.1149/1.2047547]

Manuscript submitted September 10, 2004; revised manuscript received June 8, 2005.
Available electronically September 30, 2005.

HgSe is a II-VI compound with possible applications in optoelectronics: IR detectors, IR emitters, tunable lasers, and thermoelectric coolers.[1] HgSe has been formed by molecular beam epitaxy (MBE),[2] chemical bath deposition,[1,3,4] the cold traveling heater method (CTHM),[3,5] as well as MBE using GaAs substrates.[2]

The nature of HgSe as a metal or semiconductor continues to be debated, exemplified by the work of Gawlik et al.,[6] in which they determined a direct bandgap of 0.42 eV for HgSe, suggesting a semiconductor. The band structure of HgSe has been studied using Fourier transform spectroscopy by von Truchsess et al.,[7] where they concluded that HgSe is a semimetal with an inverted structure and a bulk gap of −0.274 eV. Other studies of HgSe have reported bandgaps of 1.42 eV,[3] 2.50 eV,[8] and recently a direct bandgap of 0.81 eV and an indirect bandgap of 0.45 eV were also reported for the same deposit.[1]

The electrodeposition of II-VI compounds, in general, has been reviewed.[9,10] The majority of previous compound electrodeposition work has been directed toward the formation of cadmium chalcogenides such as CdS, CdSe, and CdTe,[9,11-20] by a variety of electrodeposition methods. The electrodeposition of cadmium chalcogenides has been studied extensively,[21-26] mainly due to their possible applications in the formation of optoelectronic devices such as photovoltaics. Studies of zinc chalcogenide electrodeposition (ZnTe and ZnSe)[22,24,26] have been reported as well.

Studies of the electrodeposition of mercury chalcogenides are few,[1,3,27-31] primarily because of the differences in potentials needed to deposit Hg and the chalcogenides, electrochemically. Hg is a noble metal and begins to deposit from solutions of Hg^{2+} at a fairly positive potential (E^o = 0.851 V vs standard hydrogen electrode). Chalcogenide reduction is much less noble, and generally displays slow deposition kinetics,[30,32-34] typically depositing below 0.0 V in neutral solutions.

The fastest and simplest method for compound electrodeposition is codeposition, where both elements are deposited simultaneously from the same solution. This has been used with good results in the commercial formation of CdTe deposits for photovoltaics, for instance. In general, the method involves use of a metal ion that deposits at potentials below those needed to deposit the chalcogenide. A low concentration of the chalcogenide can be used, which is deposited at an overpotential. However, this same potential corresponds to an underpotential for the metal ion. At underpotentials, an atomic layer of one element deposits on a second, at a potential prior to (under) that needed to deposit the element on itself. This happens because of the free energy of compound formation, the formation of a surface compound or alloy. When the surface is covered, the driving force for formation of the compound is no longer present. In the case of codeposition, the low concentration chalcogenide will limit the deposition rate, while the metal quickly deposits at an underpotential on top of any chalcogenide atoms that deposit, as the metal is present at a significant excess. This means that each chalcogenide atom reacts with one metal ion, resulting in control of the deposit stoichiometry, 1:1. In the case of codeposition of the Hg chalcogenides, however, Hg is more noble than the chalcogenide, not the other way around, and the chalcogenide underpotential deposit (UPD) on Hg has slow kinetics, making it difficult to achieve 1:1 stoichiometry.

The work in this group focuses on the development of electrochemical atomic-layer epitaxy (EC-ALE) for the formation of compound semiconductor thin films.[35-38] It is the electrochemical analog of atomic layer epitaxy (ALE)[39-42] or atomic layer deposition (ALD),[43-48] both of which are gas- or vacuum-based methods for the formation of compounds an atomic layer at a time, using surface-limited reactions. As noted, UPD is an electrochemical surface-limited reaction and is used in EC-ALE to promote monolayer-by-monolayer growth, and promote epitaxy. Most EC-ALE studies have involved growth of II-VI compounds,[16,38,49-52] although some III-V[53] and IV-VI[54-56] compounds have also been formed. The III-V compounds InAs[53] and InSb have been formed, and some initial studies into GaAs and GaSb deposition have been performed.[57] Recently, IV-VI compounds such as PbSe and PbTe and their superlattices (PbSe/PbTe)[54-56] have also been formed using EC-ALE. We report here the first studies of the formation of HgSe using EC-ALE.

Experimental

The deposition system used here for the EC-ALE formation of thin films has been described previously.[38,58,59] Basically, it consists of pumps, valves, cell, and a potentiostat, all computer controlled using a program written in Lab View. The pump heads, valves, and tubing were confined inside an N_2-purged Plexiglass box to limit oxygen, which can affect deposit quality.

The electrochemical flow cell was of a thin-layer design, to promote laminar flow over the deposit. A gasket placed between a Au on glass substrate and an ITO auxiliary electrode defined the deposition area of 3.25 cm^2. The gaskets were generally silicon rubber, which provided a good seal. A transparent ITO auxiliary electrode was used and allowed the deposition process to be visually followed. The reference electrode, Ag/AgCl (3M NaCl) (Bioanalytical Systems, Inc., West Lafayette, IN), was positioned at the cavity outlet to limit contamination.[59]

Solutions used included pH 2, 0.2 mM $HgCl_2$, complexed with

* Electrochemical Society Active Member.
z E-mail: Stickney@chem.uga.edu

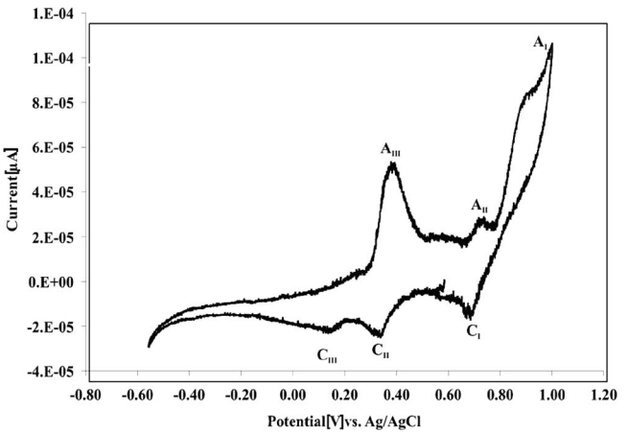

Figure 1. Cyclic voltammogram of 0.2 mM Hg^{2+}, pH 2.0 on Au. Scan rate = 5 mV/s, Au electrode surface area = 3.25 cm^2.

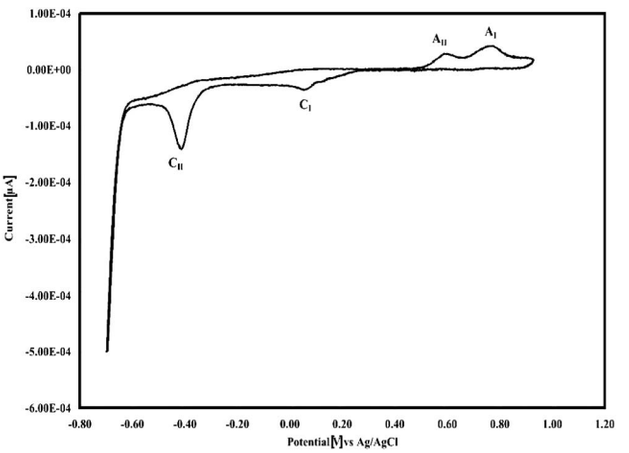

Figure 2. Cyclic voltammogram of 0.25 mM $HSeO_3^-$, pH 3.0 on Au. Scan rate = 5 mV/s, Au electrode surface area = 3.25 cm^2.

10 mM ethylenediaminetetraacetic acid (EDTA), as well as 0.25 mM $HSeO_3^-$, pH 3, and a pH 4.0 blank solution. Solution pH was adjusted with H_2SO_4 and a supporting electrolyte of 0.5 M Na_2SO_4 was used in all solutions. The water used was supplied from a Nanopure water filtration system (Barnstead, Dubuque, IA) hooked to the house distilled water system. The chemicals were reagent grade or better.

Substrates were glass microscope slides with a 3 nm Ti adhesion layer and 600 nm of Au. Substrates were formed by first etching the glass in 15% HF for 60 s, then rinsed in ultrapure water, and inserted into the vapor deposition chamber. They were then annealed at 400°C for 12 h under a 10^{-6} torr vacuum before deposition, as well as during deposition.[54] Each resulting substrate was etched in concentrated nitric acid for 5 min and then annealed in a hydrogen flame prior to use.

The EC-ALE cycle used for film growth on the Au substrates was as follows: the $HSeO_3^-$ solution was first pumped into the cell for 2 s (50 mL/min). The solution was then held for 15 s, without pumping, for deposition, and then flushed from the cell by pumping the blank solution for 3 s. This was followed by a 2 s fill with the Hg^{2+} solution, and holding for 15 s for deposition. The cycle was then completed by flushing the Hg^{2+} solution from the cell with 3 s of the blank, and refilling with the $HSeO_3^-$ solution. This cycle, ideally, results in the deposition of one monolayer of the compound. The thickness of a deposit was then determined by the number of times the cycle was performed.

The deposits were initially inspected with a Jenavert metallographic microscope. The thickness was measured using a single wavelength Ellipsometer (Sentech SE 400). Glancing angle X-ray diffraction patterns were acquired on a PAD V diffractometer with Cu Kα radiation (λ = 1.5418Δ), equipped with a thin film attachment. Electron probe microanalysis (EPMA) was run on a Joel 8600 wavelength dispersive scanning electron microprobe. AFM studies were performed using a Dimension 3100 (Digital Instruments, Santa Barbara, CA). Absorption measurements were performed in reflection mode, using a Fourier transform infrared (FTIR) spectrophotometer (Bruker FTS-66v, Bruker Optics, Inc.).

Results and Discussion

The starting potentials for steps in the development of an EC-ALE program are usually determined from cyclic voltammograms. Typical voltammograms for Hg^{2+} and $HSeO_3^-$ on Au on glass substrates are shown in Fig. 1 and 2, respectively. The Hg scan (Fig. 1) was started negatively from 0.7 V and shows two reduction features, C_{II} and C_{III}, in the initial negative going scan. The first peak appears to be a UPD feature while the second is presumed to be bulk Hg deposition. On the subsequent positive going scan, there were three major oxidation features, A_{III}, A_{II}, and A_I. A_{III} is bulk Hg oxidation, suggesting that the formal potential is between A_{III} and C_{III}, or about 0.25 V for this solution. This formal potential was the result of complexation of the Hg^{2+} ions with EDTA, which shifts the bulk deposition potential from about 0.7 V. A_{II} is probably UPD stripping, but could also be the dissolution of Hg from an amalgam (an alloy of Au and Hg). The difference between UPD and alloy formation is simply that in an alloy the depositing metal can go subsurface. The driving forces are the same for both: a decrease in free energy. The large oxidative current above 0.8 V, A_I, was oxidation of EDTA. Upon reversing to a negative going scan again, a small reduction peak, C_I, is evident, and may be a UPD feature. It has been noted in these and other studies of Hg deposition that the voltammetry can be quite variable, probably the result of the time dependence of amalgam formation and stripping. This has led to increased uncertainty in the assignments just described.

The negative going $HSeO_3^-$ scan, shown in Fig. 2, was started at 0.4 V and showed an initial reduction feature at 0.25 V with a peak at 0.05 V (C_I). In addition, there are reduction features at −0.4 (C_{II}) and −0.7 V. In the subsequent positive going scan, oxidation begins about 0.4 V, and results in two peaks at 0.6 V (A_{II}) and 0.75 V (A_I). The feature at −0.7 V is hydrogen evolution, but may also involve some selenium reduction to selenide. C_I has the appearance of a drawn out UPD peak, or a surface-limited process, as does C_{II}. C_{II}, however, is larger than expected for a normal UPD process, where the formation of a single atomic layer of an element would be expected. Previous studies[60,61] have shown this peak to correspond to the formation of a couple of monolayers of Se, probably due to the nature of the Se film. Bulk Se is normally composed of chains of chalcogenide atoms, held together by van der Waals forces.[62] Electron transfer may limit the rate of deposition after the first couple of monolayers, accounting for C_{II},[60,63] because the initial atomic layer deposition was on the Au substrate, while subsequent deposition occurs on bulk Se. In addition, given that the formal potential for $HSeO_3^-$/Se is about 0.4 V, both C_I and C_{II} are overpotential peaks, not underpotential peaks. This is again the result of slow deposition kinetics for Se in general. Peak A_{II} corresponds to bulk Se oxidation, but is smaller than expected, a result of the reduction of most bulk Se during the hydrogen evolution reaction at −0.7 V, forming a soluble selenide species which diffuses away. Peak A_I corresponds to oxidation of the first Se atomic layer, or UPD stripping.

From experience, it has been shown that by keeping the potential above −0.4 V, most bulk Se deposition can be avoided. However, given that the formal potential for Se deposition is about 0.4 V, thermodynamically, bulk Se is stable at any potential less than 0.4 V, and peaks C_I and C_{II} are not classic UPD features, but instead

Table I. Thickness and stoichiometry data of HgSe deposits.

Sample	No. of cycles	*E* (V) vs Ag/AgCl	Se/Hg ratio	Th (nm)
HgSe6/11/032	50	Se −0.18 and Hg 0.15	1.11	15.64
HgSe6/16/03	50	Se −0.30 and Hg −0.20	1.13	24.95
HgSe6/4/03	100	Se −0.60 and Hg −0.60	1.02	33.03
HgSe6/5/03	100	Se −0.25 and Hg −0.20	0.99	45.74
HgSe6/5/032	50	Se −0.28 and Hg −0.20	0.90	11.65
HgSe6/8/03	50	Se −0.30 and Hg −0.25	0.89	26.50
HgSe6/9/03	100	Se −0.30 and Hg −0.25	0.99	34.51
HgSe6/9/031	200	Se −0.30 and Hg −0.25	0.99	66.72
HgSe6/9/032	200	Se −0.25 and Hg −0.20	0.97	59.40

are formed at overpotentials.[15,60,64-67] Use of such overpotentials for EC-ALE cycles, where the deposition is predominantly surface-limited, has been successful. Drawbacks are that some small amount of bulk chalcogenide is being deposited, so the deposition time used for Se makes a difference in the amount of bulk Se deposited, as it is not a purely surface-limited process. This factor also increases the influence of mass transfer on the deposit, where for purely surface-limited processes the importance of mass transfer should be minimal.

From the voltammetry shown in Fig. 1 and 2, starting potentials for the initial EC-ALE cycle program were selected. For the Se step, −0.15 V (Fig. 2) was used, so that the first atomic layer "UPD" peak, C_I, would be included, while avoiding C_{II}, where multiple layers of Se might be deposited. The initial Hg deposition potential selected was 0.275 V, just prior to initiation of bulk Hg formation. The initial HgSe cycle started with a 2 s Hg solution fill step at 0.275 V, followed by 15 s of deposition with no solution flow. The cell was then rinsed through with blank for 3 s, filled for 2 s with the $HSeO_3^-$ solution, and held at −0.15 V for 15 s for deposition. Finally, the $HSeO_3^-$ solution was flushed from the cell with 3 s of the blank. The intent was for each cycle to result in the deposition of a HgSe compound ML, with the deposit thickness increasing linearly with the number of cycles.

By following the current time traces for the deposition, it was evident that the depositions dropped off over the first 10 or so cycles. The LabView program used to control the depositions allowed potentials to be shifted from cycle to cycle. Experience has shown that potentials used to form atomic layers on the Au substrate are frequently not the potentials needed to deposit atomic layers after the deposit has started to grow. This appears to be related to differences in the thermodynamics of UPD on the substrate metal vs on the growing compound. By shifting the potentials after each cycle, for the first 5–10 cycles, steady-state potentials can generally

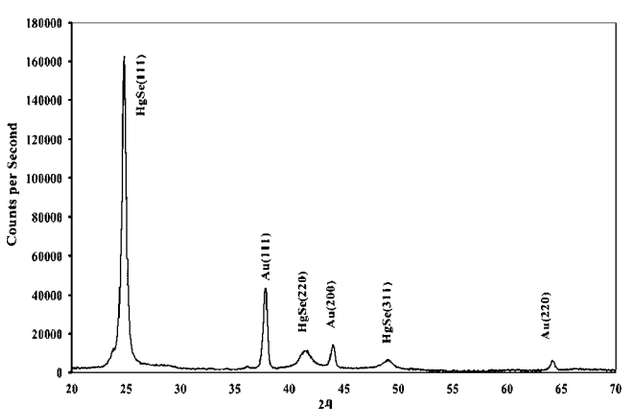

Figure 3. XRD diffraction pattern for HgSe 50803, showing the present HgSe peaks. The elemental peaks for Hg and Se were not present.

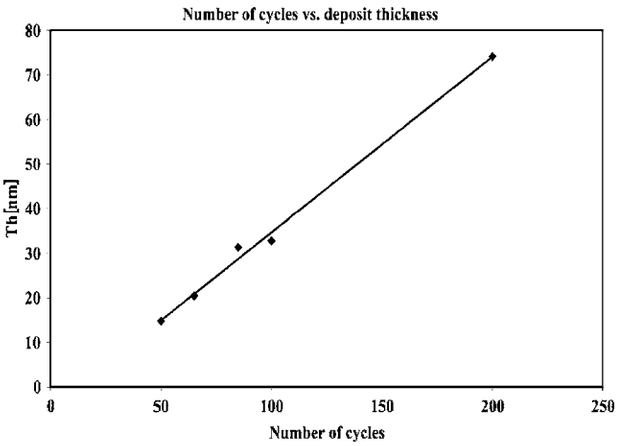

Figure 4. Thickness plot of different number of cycles of HgSe deposits.

be reached, potentials which do not need to be shifted, yet maintain deposition at 1 ML/cycle. Linear or logarithmic changes in potential can be used for the first few cycles, to better maintain consistent deposition from cycle to cycle. The largest potential steps are usually needed after the first cycle, as electronic effects from the Au substrate drop off rapidly as the compound layers are formed. The steady state potentials used for the first deposits were 0.15 V for Hg and −0.18 V for Se.

The principle of EC-ALE is that underpotentials are used to promote 2D or layer-by-layer growth. STM studies of Hg deposition on Au suggest that UPD does occur.[3,8,29,32,34] Current time traces observed in the formation of HgSe suggested that Hg deposition occurred in a UPD-like surface-limited reaction, while from current time traces, Se deposition appears to have two components, a fast surface-limited deposition, along with a small background current attributable to the slow deposition of bulk Se. This is expected, given the discussion of Se deposition above. To try and better optimize film quality, a series of deposits were formed using different steady-state potentials. Deposit quality was monitored using EPMA for stoichiometry (Table I), XRD for structure (Fig. 3), and coulometry for elemental coverages.

Coverages from coulometry at the steady-state potentials averaged 0.37 ML for Hg and 0.52 ML for Se, where one atom per Au (111) surface atom corresponds to 1.0 ML. Deposits were Se-rich as

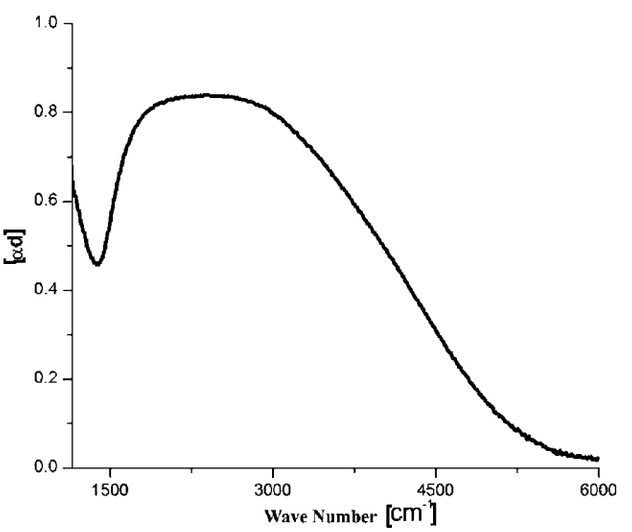

Figure 5. HgSe absorption spectra with a dip around 1500 cm^{-1}.

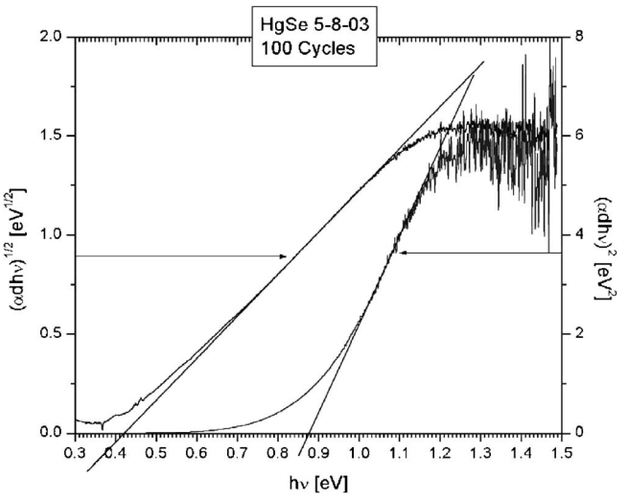

Figure 6. Plot for the indirect and direct bandgap determination using Eq. 2.

shown in Table I, as suggested by coulometry. Deposit thicknesses were determined using ellipsometry and indicated a linear increase in thickness with the number of cycles performed, as expected (Fig. 4), suggesting that the deposit thicknesses were a direct function of the number of cycles, as expected for an ALE process.

An XRD pattern for a HgSe deposit is shown in Fig. 3. From the diffraction pattern, peaks corresponding to the (111), (200), (220), (311), (222), (400), and (331) planes of HgSe were evident, matching the JCPDS 8-469 card and indicating a zinc blende deposit. Only peaks for HgSe and the Au substrate were evident in the XRD, no elemental peaks for Hg or Se were observed. The peak pattern showed a strong (111) texture.

The Scherrer equation 1 was used to calculate grain size

$$D = \frac{K\lambda}{B \cos \theta} \quad [1]$$

where $K = 0.9$, λ is the wavelength of 1.5418 Å, B is the full width at half-maximum in radians, and θ is the Bragg diffraction angles.[1] An average grain size of 42.5 nm was determined for the deposits. Note, however, that the films were only about 70 nm thick.

A room-temperature absorption measurement of a HgSe deposit over an absorption range of 6000–1500 cm^{-1} is shown in Fig. 5. The bandgap was determined from a plot of α^2 vs $h\nu$ using Eq. 2

$$\alpha(h\nu) = A(h\nu - E_g)^{1/2} \quad [2]$$

where $\alpha(h\nu)$ is the absorption coefficient, $h\nu$ is the photon energy, A is a proportionality constant, and E_g is the direct energy gap. Figure 6 shows a plot of the square of the absorption data vs energy for the 100-cycle deposit. The plot of absorption measurements showed a direct bandgap of 0.42 eV and an indirect bandgap of 0.88 eV, in good agreement with literature values of 0.45 and 0.81 eV.[1]

Conclusions

The formation of HgSe thin films by EC-ALE has been shown for the first time. The growth conditions, from current time traces, are in agreement with EPMA results, showing that deposits were selenium-rich when positive Se potentials were used. The deposition mechanism for HgSe will be the subject of future STM and EQCM studies. XRD patterns showed that the HgSe deposits were polycrystalline, with a strongly preferential (111) orientation. Bandgap measurements showed the existence of direct and indirect energy gaps of 0.42 and 0.88 eV, respectively.

Acknowledgments

Financial support from the NSF divisions of Chemistry and Materials is gratefully acknowledged.

The University of Georgia assisted in meeting the publication costs of this article.

References

1. P. P. Hankare, V. M. Bhuse, K. M. Garadkar, and A. D. Jadhav, *Mater. Chem. Phys.*, **71**, 53 (2001).
2. L. Parthier, H. Wissmann, S. Luther, G. Machel, M. Schmidbauer, R. Kohler, and M. Von Ortenberg, *J. Cryst. Growth*, **175–176**, 642 (1997).
3. P. Pramanik and S. Bhattacharya, *Mater. Res. Bull.*, **24**, 945 (1989).
4. Y. Li, Y. Ding, H. Liao, and Y. Qian, *J. Phys. Chem. Solids*, **60**, 965 (1999).
5. C. Reig, Y. S. Paranchych, and V. Munoz-Sanjose, *Cryst. Growth Des.*, **2**, 91 (2002).
6. K. U. Gawlik, L. Kipp, M. Skibowski, N. Orlowski, and R. Manzke, *Phys. Rev. Lett.*, **78**, 3165 (1997).
7. M. von Truchsess, A. Pfeuffer-Jeschke, C. R. Becker, G. Landwehr, and E. Batke, *Phys. Rev. B*, **61**, 1666 (2000).
8. B. B. Pejova, M. Z. Najdoski, I. S. Grozdanov, and S. K. Dey, *J. Mater. Chem.*, **9**, 2889 (1999).
9. G. F. Fulop and R. M. Taylor, *Annu. Rev. Mater. Sci.*, **15**, 197 (1985).
10. G. Hodes, in *Physical Electrochemistry*, I. Rubinstein, Editor, p. 515, Marcel Dekker, New York (1995).
11. K. Rajeshwar, *Adv. Mater. (Weinheim, Ger.)*, **4**, 23 (1992).
12. G. Hodes, *Sol. Energy Mater. Sol. Cells*, **32**, 323 (1994).
13. R. K. Pandey, S. N. Sahu, and S. Chandra, *Handbook of Semiconductor Electrodeposition*, Marcel Dekker, Inc., New York (1996).
14. B. W. Gregory, D. W. Suggs, and J. L. Stickney, *J. Electrochem. Soc.*, **138**, 1279 (1991).
15. B. M. Huang, L. P. Colletti, B. W. Gregory, J. L. Anderson, and J. L. Stickney, *J. Electrochem. Soc.*, **142**, 3007 (1995).
16. L. P. Colletti and J. L. Stickney, *J. Electrochem. Soc.*, **145**, 3594 (1998).
17. L. P. Colletti, B. H. Flowers, Jr., and J. L. Stickney, *J. Electrochem. Soc.*, **145**, 1442 (1998).
18. U. Demir and C. Shannon, *Langmuir*, **10**, 2794 (1994).
19. G. D. Aloisi, M. Cavallini, M. Innocenti, M. L. Foresti, G. Pezzatini, and R. Guidelli, *J. Phys. Chem. B*, **101**, 4774 (1997).
20. B. E. Hayden and I. S. Nandhakumar, *J. Phys. Chem. B*, **102**, 4897 (1998).
21. B. Bozzini, C. Lenardi, and N. Lovergine, *Mater. Chem. Phys.*, **66**, 219 (2000).
22. B. Bozzini, M. A. Baker, P. L. Cavallotti, E. Cerri, and C. Lenardi, *Thin Solid Films*, **361–362**, 388 (2000).
23. G. Riveros, H. Gomez, R. Henriquez, R. Schrebler, R. E. Marotti, and E. A. Dalchiele, *Sol. Energy Mater. Sol. Cells*, **70**, 255 (2001).
24. M. Neumann-Spallart and C. Konigstein, *Thin Solid Films*, **265**, 33 (1995).
25. R. Chandramohan, T. Mahalingam, J. P. Chu, and P. J. Sebastian, *Sol. Energy Mater. Sol. Cells*, **81**, 371 (2004).
26. C. Natarajan, M. Sharon, C. Levy-Clement, and M. Neumann-Spallart, *Thin Solid Films*, **237**, 118 (1994).
27. M. E. Martins, R. C. Salvarezza, and A. J. Arvia, *Electrochim. Acta*, **43**, 549 (1998).
28. D. R. Salinas, E. O. Cobo, S. G. Garcia, and J. B. Bessone, *J. Electroanal. Chem.*, **470**, 120 (1999).
29. C. Natarajan, M. Sharon, C. Levy-Clement, and M. Neumann-Spallart, *Thin Solid Films*, **257**, 46 (1995).
30. G. Mattsson, L. Nyholm, and A. Olin, *J. Electroanal. Chem.*, **377**, 149 (1994).
31. C. N. Van Huong, R. Triboulet, and P. Lemasson, *J. Cryst. Growth*, **101**, 311 (1990).
32. R. Djogic, I. Pizeta, and M. Zelic, *Anal. Chim. Acta*, **404**, 159 (2000).
33. W. Szuszkiewicz, E. Dynowska, J. Gorecka, B. Witkowska, M. Jouanne, J. F. Morhange, C. Julien, and B. Hennion, *Phys. Status Solidi B*, **215**, 93 (1999).
34. G. Mattsson, L. Nyhom, and L. M. Peter, *J. Electroanal. Chem.*, **347**, 303 (1993).
35. B. W. Gregory and J. L. Stickney, *J. Electroanal. Chem. Interfacial Electrochem.*, **300**, 543 (1991).
36. B. M. Huang, T. E. Lister, and J. L. Stickney, in *Handbook of Surface Imaging and Visualization*, A. T. Hubbard, Editor, p. 75, CRC Press, Boca Raton, FL (1995).
37. J. L. Stickney, in *Electroanalytical Chemistry*, A. J. Bard and I. Rubenstein, Editors, Vol. 21, p. 75, Marcel Dekker, New York (1999).
38. J. L. Stickney, in *Advances in Electrochemical Science and Engineering*, D. M. Kolb and R. Alkire, Editors, Vol. 7, p. 1, Wiley-VCH, Weinheim (2002).
39. S. Bedair, *Atomic Layer Epitaxy*, Elsevier, Amsterdam (1993).
40. T. F. Kuech, P. D. Dapkus, and Y. Aoyagi, *Atomic Layer Growth and Processing*, Materials Research Society, Pittsburgh (1991).
41. C. H. L. Goodman and M. V. Pessa, *J. Appl. Phys.*, **60**, R65 (1986).
42. W. Faschinger, *Phys. Scr., T*, **49B**, 492 (1993).
43. M. Leskela and M. Ritala, *Thin Solid Films*, **409**, 138 (2002).
44. E. B. Yousfi, B. Weinberger, F. Donsanti, P. Cowache, and D. Lincot, *Thin Solid Films*, **387**, 29 (2001).
45. V. Sammelselg, A. Rosental, A. Tarre, L. Niinisto, K. Heiskanen, K. Ilmonen, L.-S. Johansson, and T. Uustare, *Appl. Surf. Sci.*, **134**, 78 (1998).
46. M. Ylilammi, *Thin Solid Films*, **279**, 124 (1996).
47. J. S. Best and J. O. McCaldin, *J. Vac. Sci. Technol.*, **16**, 1130 (1979).
48. B. E. Conway, *Prog. Surf. Sci.*, **16**, 1 (1984).
49. T. L. Wade, B. H. Flowers, Jr., U. Happek, and J. L. Stickney, in *National Meeting*

of the Electrochemical Society, Spring, P. C. Andricacos, P. C. Searson, C. Reidsema-Simpson, P. Allongue, J. L. Stickney, and G. M. Oleszek, Editors, Vol. 99-9, p. 272, The Electrochemical Society, Seattle, WA (1999).
50. T. L. Wade, B. H. Flowers, Jr., R. Vaidyanathan, K. Mathe, C. B. Maddox, U. Happek, and J. L. Stickney, in *Materials Research Society*, Vol. 581, p. 145, Materials Research Society, Pittsburgh (2000).
51. J. L. Stickney, K. Varazo, L. C. Ward, M. D. Lay, and T. Sorenson, in *Encyclopedia of Surface and Colloid Science*, A. T. Hubbard, Editor, Marcel Dekker, Inc., New York (2002).
52. M. K. Mathe, S. M. Cox, B. H. Flowers, Jr., R. Vaidyanathan, L. Pham, N. Srisook, U. Happek, and J. L. Stickney, *J. Cryst. Growth*, **271**, 55 (2004).
53. T. L. Wade, L. C. Ward, C. B. Maddox, U. Happek, and J. L. Stickney, *Electrochem. Solid-State Lett.*, **2**, 616 (1999).
54. R. Vaidyanathan, J. L. Stickney, and U. Happek, *Electrochim. Acta*, **49**, 1321 (2004).
55. R. Vaidyanathan, U. Happek, and J. L. Stickney, *J. Phys. Chem. B*, To be submitted for publication.
56. R. Vaidyanathan, U. Happek, and J. L. Stickney, *Appl. Phys. Lett.*, To be submitted for publication.
57. I. Villegas and J. L. Stickney, *J. Electrochem. Soc.*, **139**, 686 (1992).
58. T. L. Wade, T. A. Sorenson, and J. L. Stickney, in *Interfacial Electrochemistry*, A. Wieckowski, Editor, p. 757, Marcel Dekker, New York (1999).
59. B. H. Flowers, Jr., M. K. Mathe, R. Vaidyanathan, N. Srisook, U. Happek, and J. L. Stickney, in *Morphological Evolution of Electrodeposits – and – Electrochemical Processing in ULSI Fabrication and Electrodeposition of and on Semiconductors IV*, P. C. Allongue, P. C. Andricacos, F Argoul, D. P. Barkey, J. C. Bradley, K. Kondo, P. C. Searson, C. Reidsma-Simpson, J. L. Stickney, and G. M. Olezek, Editors, PV 2001–08, p. 381, The Electrochemcial Society Proceedings Series, Pennington, NJ (2005).
60. B. M. Huang, T. E. Lister, and J. L. Stickney, *Surf. Sci.*, **392**, 27 (1997).
61. F. Forni, M. Innocenti, G. Pezzatini, and M. L. Foresti, *Electrochim. Acta*, **45**, 3225 (2000).
62. N. N. Greenwood and A. Earnshaw, *Chemistry of the Elements*, Pergamon Press, Oxford (1984).
63. T. E. Lister and J. L. Stickney, *Appl. Surf. Sci.*, **107**, 153 (1996).
64. W. Obretenov, U. Schmidt, W. J. Lorenz, G. Staikov, E. Budevski, D. Carnal, U. Muller, H. Siegenthaler, and E. Schmidt, *J. Electrochem. Soc.*, **140**, 692 (1993).
65. E. A. Streltsov, N. P. Osipovich, L. S. Ivashkevich, and A. S. Lyakhov, *Electrochim. Acta*, **44**, 2645 (1999).
66. E. A. Streltsov, N. P. Osipovich, L. S. Ivashkevich, A. S. Lyakhov, and V. V. Sviridov, *Electrochim. Acta*, **43**, 869 (1998).
67. M. Kemell, H. Saloniemi, M. Ritala, and M. Leskela, *Electrochim. Acta*, **45**, 3737 (2000).